respectively. The low value for the C–C–C angle of the η^2-tame six-membered chelate ring is probably caused by the substituents on C(3). The six-membered ring has a chair conformation, as shown by the torsion angles in Table X. Comparison with $(-)_{589}$-$Co(tn)_3^{3+}$ [32] and an idealized chair conformation in $Co(tn)_3^{3+}$ [32] shows that the chelate ring is flattened out by interactions between nonbonded H atoms of adjacent chelate rings.

Acknowledgment. We thank the Rhodes Trust for a Rhodes Visiting Fellowship (to C.C.) at Somerville College, Oxford, and Dr. C. K. Prout of the Chemical Crystallography Laboratory, Oxford, for diffractometer facilities.

Registry No. I, 73953-30-7; II, 73953-32-9; III, 73953-40-9; IV, 73953-33-0; $[Co(\eta^2\text{-Htame})(\eta^3\text{-tame})Cl]Cl_3\cdot 2H_2O$, 73953-34-1; $[Co(\eta^2\text{-Htame})(\eta^3\text{-tame})Br]Br_3$, 73953-35-2; $[Co(\eta^2\text{-Htame})(\eta^3\text{-tame})NCS](NCS)_2ClO_4$, 73953-38-5; $[Co(\eta^2\text{-Htame})(\eta^3\text{-tame})OH](ClO_4)_3$, 73953-41-0; $[Co(\eta^2\text{-Htame})(\eta^2\text{-tame})H_2O](ClO_4)_4$, 73953-44-3; $[Co(\eta^2\text{-Htame})(\eta^3\text{-tame})SO_4]SO_4$, 73953-46-5; $[Co(\eta^2\text{-bstame})(\eta^3\text{-tame})Cl]Cl_2$, 73953-47-6; $[Co(\eta^2\text{-actame})(\eta^3\text{-tame})CH_3COO]CH_3COOClO_4$, 73953-49-8; $Na_3Co(CO_3)_3$, 23311-39-9; tame·3HCl, 31044-82-3.

Supplementary Material Available: Observed and calculated structure factor amplitudes (Table XI) and k_{expl} of the base hydrolyses (Table XII) (23 pages). Ordering information is given on any current masthead page.

(32) R. Nagao, F. Marumo, and Y. Saito, *Acta Crystallogr., Sect. B*, **B29**, 2438 (1973).
(33) S. R. Niketić and F. Woldbye, *Acta Chem. Scand.*, **27**, 621 (1973).

Contribution from the Department of Chemistry, The University of Alberta, Edmonton, Alberta, Canada T6G 2G2

Unusual Structural and Chemical Trends within a Series of Binuclear Rhodium Carbonyl Halide Complexes and the Structure of One Member of This Series, *trans*-$[Rh_2Cl_2(CO)_2((C_6H_5)_2PCH_2P(C_6H_5)_2)_2]$

MARTIN COWIE* and STEPHEN K. DWIGHT

Received October 12, 1979

The reaction of *trans*-$[Rh_2Cl_2(CO)_2(DPM)_2]$ (DPM = $(C_6H_5)_2PCH_2P(C_6H_5)_2$) with NaBr yields initially the unusual, asymmetric species $[Rh_2Br(\mu\text{-CO})(CO)(DPM)_2][Br]$, which in solution loses CO yielding the "A-frame" species $[Rh_2Br_2(\mu\text{-CO})(DPM)_2]$. When the above reaction is carried out with KI instead of NaBr, the complex $[Rh_2I(\mu\text{-CO})(CO)(DPM)_2][I]$ is produced as the final product. These bromo- and iododicarbonyl complexes react with CO and SO_2 to yield the complexes $[Rh_2(CO)_2(\mu\text{-L})(\mu\text{-X})(DPM)_2][X]$ (L = CO, SO_2; X = Br, I). The dichloromonocarbonyl species $[Rh_2Cl_2(\mu\text{-CO})(DPM)_2]$ was prepared by refluxing *trans*-$[Rh_2Cl_2(CO)_2(DPM)_2]$ in toluene. Reaction of the chloro- and bromomonocarbonyl complexes with an excess of CO yields $[Rh_2(CO)_2(\mu\text{-CO})(\mu\text{-X})(DPM)_2][X]$ (X = Cl, Br). With the dichloromonocarbonyl species, slow stepwise addition of CO results instead in the formation of *trans*-$[Rh_2Cl_2(CO)_2(DPM)_2]$. Reaction of both monocarbonyl species with SO_2 produces an equimolar mixture of $[Rh_2X_2(\mu\text{-}SO_2)(DPM)_2]$ and $[Rh_2(CO)_2(\mu\text{-}SO_2)(\mu\text{-X})(DPM)_2][X]$ (X = Cl, Br). The tricarbonylbromo species loses one terminal carbonyl ligand slowly in solution under an N_2 stream, yielding the above asymmetric bromo species, but does not lose CO in the solid state under vacuum. The analogous iodotricarbonyl complex does not lose CO even in solution. The bromo–SO_2 adduct loses both CO ligands in solution under an N_2 flush, yielding $[Rh_2Br_2(\mu\text{-}SO_2)(DPM)_2]$, whereas the iodo–$SO_2$ adduct loses neither CO nor SO_2. *trans*-$[Rh_2Cl_2(CO)_2(DAM)_2]$ (DAM = $(C_6H_5)_2AsCH_2As(C_6H_5)_2$) undergoes iodide exchange to give a mixture of *trans*-$[Rh_2I_2(CO)_2(DAM)_2]$ and $[Rh_2(I)(\mu\text{-CO})(CO)(DAM)_2][I]$. These iodo–DAM species react with CO and SO_2, yielding $[Rh_2(CO)_2(\mu\text{-L})(\mu\text{-I})(DAM)_2][I]$ (L = CO, SO_2). The CO reaction is reversible in solution, but the SO_2 reaction is not. The structure of *trans*-$[Rh_2Cl_2(CO)_2(DPM)_2]$ has been determined by X-ray crystallography, verifying that it has a dimeric formulation essentially isostructural with its bis(diphenylarsino)methane analogue. The complex *trans*-$[Rh_2Cl_2(CO)_2(DPM)_2]$ crystallizes in the space group $P\bar{1}$ (No. C_i^1) with a = 11.054 (1) Å, b = 12.564 (1) Å, c = 10.3191 (9) Å, α = 99.899 (6)°, β = 115.708 (7)°, and γ = 65.082 (7)° with Z = 1. On the basis of 3368 unique reflections the structure was refined by full-matrix, least-squares techniques to R = 0.037 and R_w = 0.069. The Rh–Rh separation is 3.2386 (5) Å, and the two parallel rhodium square planes are inclined to the Rh–Rh vector by ca. 75.9°.

Introduction

We have recently been interested in the reactions of binuclear rhodium complexes with small molecules[1–6] and as part of our studies in this area have been investigating the chemistries of *trans*-$[Rh_2Cl_2(CO)_2(DPM)_2]$,[7] **1**, and *trans*-$[Rh_2Cl_2(CO)_2(DAM)_2]$,[7] **2**. These dichlorodicarbonyl complexes have been shown to react with small molecules yielding species[6,8] which seem to contain ketonic[9] carbonyl ligands. Since the stabilities of ketonic carbonyl complexes have been found to differ with the DPM and DAM ligands,[6,10,11] we undertook an investigation into the possible effects of varying the halide ligands on the stabilities of these complexes. We therefore attempted the preparations of the *trans*-dibromo- and -diiodo–DPM complexes and the *trans*-diiodo–DAM complex, none of which had been reported.

During this study it also became apparent to us that it was of interest to obtain an accurate structural determination of complex **1**. Although, on the basis of powder diffraction studies,[12] it seemed that complex **1** was isomorphous with complex **2**, whose structure has been determined,[13] significant differences in their chemistries had led us to question the extent of their similarities. It had been noted, for example, that

(1) Cowie, M.; Mague, J. T.; Sanger, A. R. *J. Am. Chem. Soc.* **1978**, *100*, 3628.
(2) Cowie, M. *Inorg. Chem.* **1979**, *18*, 286.
(3) Cowie, M.; Dwight, S. K.; Sanger, A. R. *Inorg. Chim. Acta* **1978**, *31*, L407.
(4) Cowie, M.; Dwight, S. K. *Inorg. Chem.* **1979**, *18*, 1209.
(5) Cowie, M.; Dwight, S. K. *Inorg. Chem.* **1979**, *18*, 2700.
(6) Cowie, M.; Dwight, S. K. *Inorg. Chem.* **1980**, *19*, 209.
(7) Abbreviations used: DPM, bis(diphenylphosphino)methane; DAM, bis(diphenylarsino)methane; Me, methyl; Et, ethyl.
(8) Cowie, M.; Dwight, S. K. *J. Organomet. Chem.*, in press.
(9) The term ketonic carbonyl refers to a carbonyl ligand which bridges two metal centers which are not bonded to each other.
(10) Colton, R.; McCormick, M. J.; Pannan, C. D. *J. Chem. Soc., Chem. Commun.* **1977**, 823.
(11) Brown, M. P.; Keith, A. N.; Manojlovic-Muir, L.; Muir, K. W.; Puddephatt, R. J.; Seddon, K. R. *Inorg. Chim. Acta* **1979**, *34*, L223.
(12) Mague, J. T.; Mitchener, J. P. *Inorg. Chem.* **1969**, *8*, 119.
(13) Mague, J. T. *Inorg. Chem.* **1969**, *8*, 1975.

0020-1669/80/1319-2500$01.00/0

Table I. Spectral Data for the Complexes

no.	complex	Infrared abs maxima,[a] cm^{-1}	$^{31}P\{^1H\}$ NMR chem shifts,[b] ppm
3	$[Rh_2Br(\mu\text{-}CO)(CO)(DPM)_2][Br]$	1958 (s), 1800 (m)	25.0 (multiplet)
4a	$[Rh_2Cl_2(\mu\text{-}CO)(DPM)_2]$	1745 (s)	19.7 (115.9 Hz)
4b	$[Rh_2Br_2(\mu\text{-}CO)(DPM)_2]$	1745 (s)	19.4 (114.7 Hz)
5	$[Rh_2I(\mu\text{-}CO)(CO)(DPM)_2][I]$	1955 (s), 1810 (m)	21.5 (multiplet)
6,7	$[Rh_2I_2(CO)_2(DAM)_2]$	1965 (sh), 1940 (s), 1820 (m)	
9a	$[Rh_2(CO)_2(\mu\text{-}CO)(\mu\text{-}Cl)(DPM)_2][Cl]$[c,d]	2004 (m), 1960 (s), 1868 (m)	29.8 (94.0)
9b	$[Rh_2(CO)_2(\mu\text{-}CO)(\mu\text{-}Br)(DPM)_2][Br]$	2005 (m), 1968 (s), 1865 (m)	28.7 (93.8)
9c	$[Rh_2(CO)_2(\mu\text{-}CO)(\mu\text{-}I)(DPM)_2][I]$	1990 (sh), 1970 (s), 1860 (m)	26.6 (92.7)
10a	$[Rh_2(CO)_2(\mu\text{-}SO_2)(\mu\text{-}Cl)(DPM)_2][Cl]$[d]	2010 (s), 1980 (sh), 1230 (m), 1070 (m)	24.5 (91.6)
10b	$[Rh_2(CO)_2(\mu\text{-}SO_2)(\mu\text{-}Br)(DPM)_2][Br]$	2005 (s), 1970 (sh), 1230 (m), 1085 (m)	27.0 (90.6)
10c	$[Rh_2(\mu\text{-}SO_2)(\mu\text{-}I)(CO)_2(DPM)_2][I]$	2005 (m), 1990 (s), 1210 (m), 1065 (m)	26.0 (90.3)
11	$[Rh_2(CO)_2(\mu\text{-}CO)(\mu\text{-}I)(DAM)_2][I]$	2005 (m), 1958 (s), 1860 (m)	
12	$[Rh_2(CO)_2(\mu\text{-}SO_2)(\mu\text{-}I)(DAM)_2][I]$	1985 (s), 1205 (m), 1065 (m)	
13a	$[Rh_2Cl_2(\mu\text{-}SO_2)(DPM)_2]$	1191 (m), 1063 (s)	19.6 (113.5)
13b	$[Rh_2Br_2(\mu\text{-}SO_2)(DPM)_2]$	1190 (m), 1060 (s)	21.1 (113.6)

[a] Infrared spectra run as Nujol mulls on KBr plates. Abbreviations: s, strong; m, medium; w, weak; sh, shoulder. [b] $^{31}P\{^1H\}$ NMR chemical shifts are relative to H_3PO_4 (downfield positive), coupling constants ($|^1J_{Rh-P} + {}^xJ_{Rh-P}|$) are given in parentheses. [c] References 1 and 29. [d] Reference 6.

ketonic carbonyl complexes of Pd[10] and Pt[11] were more stable with DAM than with DPM, whereas our work indicated the opposite was true with rhodium.[6] The obvious difference in these ligands lies in their ligand bites owing to the greater size of As compared to P. It was therefore deemed important to obtain information on the effects of these bridging ligands on the metal–metal distances and the subsequent effect on the stability of the ketonic carbonyl species.

The extreme insolubility of **1** compared with **2** had also caused us to question the extent of their structural similarities. Furthermore, we have reported[3,6] the preparation of an isomer of **1** which we believe to be the *cis*-dichlorodicarbonyl species and because of its differing solubility and chemistry with CO compared to the trans compound we wanted to make structural comparisons of these isomers. Hence when a reaction of **1** with CS_2 resulted in the serendipitous crystallization of complex **1**,[14] we undertook its structural determination for the above mentioned reasons.

In this paper we report the structure of complex **1** and the characterization of the unexpected series of products obtained by halide exchange in complexes **1** and **2** and their subsequent reactions with SO_2 and CO.

Experimental Section

All solvents were dried and degassed prior to use and all reactions carried out under an atmosphere of dinitrogen. *trans*-$[Rh_2Cl_2(CO)_2(DPM)_2]$ and *trans*-$[Rh_2Cl_2(CO)_2(DAM)_2]$ were prepared by the reported methods.[12] Infrared spectra were recorded on a Perkin-Elmer Model 467 spectrometer using Nujol mulls on KBr plates, NMR spectra were recorded on a Bruker HFX-90 NMR spectrometer, and conductivity measurements were carried out by using a Model 31 Yellow Springs Instrument conductivity bridge with 1×10^{-3} M solutions. Elemental analyses were performed within the department.

Halide-Exchange Reactions. Typically 0.100 g of $[Rh_2Cl_2(CO)_2(DPM)_2]$ was suspended in 15 mL of CH_2Cl_2, and to this was added a fivefold excess of the halide salt (NaBr, KI), in a minimum volume of methanol. After ca. 12 h, the solution was concentrated to about 5 mL and then precipitated with diethyl ether. The product was washed with water and then diethyl ether and dried under vacuum. The products were recrystallized from CH_2Cl_2 and diethyl ether. Typically the yields were about 70%. Anal. Calcd for $[Rh_2Br_2(CO)(DPM)_2]$, $C_{51}H_{44}Br_2O_1P_4Rh_2$: C, 52.70; H, 3.81; Br, 13.7. Found: C, 52.3; H, 3.70; Br, 13.0. Calcd for $[Rh_2I_2(CO)_2(DPM)_2]$, $C_{52}H_{44}I_2O_2P_4Rh_2$: C, 48.62; H, 3.45. Found: C, 48.25; H, 3.51. See Table I for spectral data.

Preparation of Monocarbonyl Species. A CH_2Cl_2 solution of $[Rh_2Br_2(CO)_2(DPM)_2]$ undergoes CO loss at room temperature over a period of 24 h or on refluxing for 2 h, yielding $[Rh_2Br_2(CO)(DPM)_2]$. The analogous chloro complex, $[Rh_2Cl_2(CO)(DPM)_2]$, was obtained as a red species in solution on refluxing a toluene suspension of *trans*-$[Rh_2Cl_2(CO)_2(DPM)_2]$ for 2 h. Crystallization of both monocarbonyl species was from methylene chloride/diethyl ether.

Reactions with SO_2 and CO. (i) Dicarbonyl Species. Typically 0.100 g of $[Rh_2X_2(CO)_2(DPM)_2]$ or $[Rh_2X_2(CO)_2(DAM)_2]$ (X = Cl, Br, I) in 15 mL of CH_2Cl_2 was treated with SO_2 or CO for 10 min, the volume was reduced under a stream of the reactant gas to about 7 mL, and then the products were precipitated with diethyl ether saturated with the reactant gas. Yields of the expected products, $[Rh_2(CO)_2(\mu\text{-}L)(\mu\text{-}X)(DPM)_2][X]$ (L = CO, SO_2; X = Cl, Br, I), averaged ca. 75%. The reversibility of the CO and SO_2 reactions was studied by dissolving the products of these reactions in CH_2Cl_2 and bubbling N_2 through the solution for up to 48 h.

(ii) Monocarbonyl Species. Typically 200 mg of sample was dissolved in 2 mL of CD_2Cl_2 and the reactant gas introduced a bubble at a time. The $^{31}P\{^1H\}$ NMR spectra were recorded, at −50 °C, after each addition of gas until no significant changes were observed. The infrared spectra were recorded at room temperature in an analogous manner using 200 mg of sample in 20 mL of CH_2Cl_2.

Crystallization of *trans*-$[Rh_2Cl_2(CO)_2(DPM)_2]$. To a suspension of 0.100 g of (0.091 mmol) of the yellow *trans*-$[Rh_2Cl_2(CO)_2(DPM)_2]$ in 15 mL of CH_2Cl_2 was added 15 mL of CS_2. After about 1 h, diethyl ether was added to induce crystallization from the clear red solution. The red solid was redissolved in 15 mL of CH_2Cl_2 from which well-formed yellow crystals were obtained by diethyl ether diffusion. These crystals were analyzed chemically and spectrally as the starting material, *trans*-$[Rh_2Cl_2(CO)_2(DPM)_2]$.

Data Collection. A clear yellow plate of *trans*-$[Rh_2Cl_2(CO)_2(DPM)_2]$ was mounted on a glass fiber. Preliminary film data showed $\bar{1}$ Laue symmetry and no systematic absences, consistent with the space groups $P1$ and $P\bar{1}$. The centrosymmetric space group $P\bar{1}$ was chosen and later verified by the successful refinement of the structure with acceptable positional parameters, thermal parameters and agreement indices, and the location of all hydrogen atoms in the difference Fourier syntheses. Accurate cell parameters were obtained by a least-squares analysis of the setting angles of 12 carefully centered reflections chosen from diverse regions of reciprocal space ($60° < 2\theta < 70°$; Cu Kα radiation) and obtained by using a narrow X-ray source (see Table II for pertinent crystal data). A cell reduction failed to show the presence of higher symmetry. The reduced cell is reported.[15]

Data were collected on a Picker four-circle automated diffractometer equipped with a scintillation counter and pulse-height analyzer, tuned to accept 90% of the Cu Kα peak. Background counts were measured at both ends of the scan range with stationary crystal and counter. The intensities of three standard reflections were measured every 100 reflections, and four additional standards were measured three times a day. All remained constant to within 1% of the mean throughout the data collection.

(14) Other efforts to obtain satisfactory single crystals of *trans*-$[Rh_2Cl_2(CO)_2(DPM)_2]$ failed due to its insolubility.

(15) The cell reduction was performed by using a modification of TRACERA II by S. L. Lawson. See: Lawson, S. L.; Jacobson, R. A. "The Reduced Cell and Its Crystallographic Applications", USAEC Ames Laboratory Report IS-1141; Iowa State University: Ames, Iowa, Apr 1965.

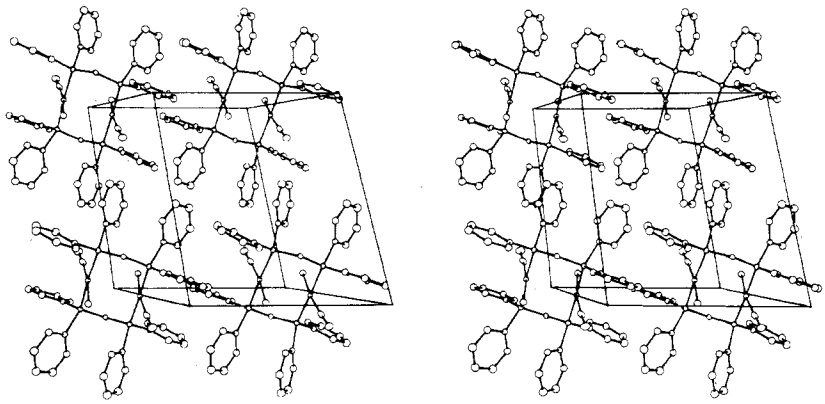

Figure 1. A stereoview of the unit cell of *trans*-$[Rh_2Cl_2(CO)_2(DPM)_2]$. The molecules for four adjacent cells in the plane at the rear of the view are drawn to show the packing interactions. The z axis is horizontal to the right, the y axis runs from bottom to top, and the x axis goes into the page. 20% vibrational ellipsoids are used on this and all other drawings unless otherwise noted. Methylene hydrogen atoms are drawn artificially small on all drawings.

Table II. Summary of Crystal Data and Intensity Collection

compd	$Rh_2Cl_2(CO)_2(DPM)_2$
formula	$C_{52}H_{44}Cl_2O_2P_4Rh_2$
fw reduced cell parameters	1101.54 amu
a	11.0542 (11) Å
b	12.5640 (10) Å
c	10.3191 (9) Å
α	99.899 (6)°
β	115.708 (7)°
γ	65.082 (7)°
Z	1
density	1.562 g·cm^{-3} (calcd)
	1.565 (5) g·cm^{-3} (exptl by flotation)
space group	$P\bar{1}$ (No. C_i^1)
cryst dimens	0.346 × 0.555 × 0.077 mm
cryst vol	0.0094 mm^3
cryst shape	triclinic prism with faces of the form {110}, {010}, and {001}
temp	20 ± 2 °C
radiatn	Cu Kα (λ 1.540 562 Å) filtered with 0.5 mil thick nickel foil
μ	85.439 cm^{-1}
range in abs cor factors (applied to F_o^2)	0.140–0.567
receiving aperture	4 × 4 mm, 30 cm from crystal
takeoff angle	4.1°
scan speed	2° in 2θ/min
scan range	1.00° below $K\alpha_1$ to 1.00 above $K\alpha_2$
bkgd counting	10 s ($3° \leq 2\theta \leq 60°$)
	20 s ($60° < 2\theta \leq 120°$)
2θ limits	3.0–120.0°
final no. of variables	113
unique data used	3368
error in observn of unit wt	1.866
R	0.037
R_w	0.069

The intensities of 3505 unique reflections ($3° \leq 2\theta \leq 120°$) were measured by using nickel-filtered Cu Kα radiation. Data were processed in the usual manner with a value of 0.05 for p.[16] Absorption corrections were applied to the data by using a Gaussian integration.[17]

Structure Solution and Refinement. The position of the independent Rh atom was obtained from a sharpened Patterson synthesis. Subsequent refinements and difference Fourier calculations led to the location of all other atoms. Atomic scattering factors were taken from Cromer and Waber's[18] tabulations for all atoms except hydrogen for which the values of Stewart et al.[19] were used. Anomalous dispersion terms[20] for Rh, Cl, and P were included in F_c. All carbon atoms of the phenyl rings were refined as rigid groups having D_{6h} symmetry and C–C distances of 1.392 Å. The hydrogen atoms were included as fixed contributions and were not refined. Their idealized positions were calculated from the geometries about their attached carbon atoms by using C–H distances of 0.95 Å. Hydrogen atoms were assigned isotropic thermal parameters of 1 Å^2 greater than their attached carbon atom. All other nongroup atoms were refined individually with anisotropic thermal parameters.

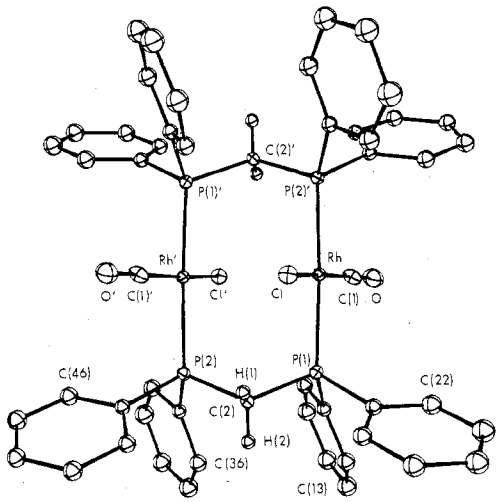

Figure 2. A perspective view of *trans*-$[Rh_2Cl_2(CO)_2(DPM)_2]$ showing the numbering scheme. The numbering of the phenyl carbons starts at the carbon bonded to phosphorus and increases sequentially around the ring.

The final model with 115 parameters varied converged to $R = 0.037$ and $R_w = 0.069$.[21] In the final difference Fourier map all of the highest 20 peaks were in the vicinity of the phenyl rings (0.91–0.54 e/Å^3). A typical carbon atom on earlier syntheses had an electron density of about 7.7 e/Å^3 The final positional parameters of the individual nonhydrogen atoms and the phenyl groups are given in Tables III and IV, respectively. The derived hydrogen positions and their thermal parameters, the root-mean-square amplitudes of vibration of individual nonhydrogen atoms, and a listing of observed and calculated strucure factor amplitudes used in the refinements are available.[22]

(16) Doedens, R. J.; Ibers, J. A. *Inorg. Chem.* **1967**, *6*, 204.
(17) Besides local programs and some kindly supplied by J. A. Ibers, the following were used in the solution and refinement of the structure: FORDAP, the Fourier summation program by A. Zalkin; SFLS-5, structure factor and least-squares refinement by C. J. Prewitt; ORFFE, for calculating bond lengths, angles and associated standard deviations by W. Busing and H. A. Levy; ORTEP, plotting program by C. K. Johnson; AGNOST, the absorption and extinction program from Northwestern University.
(18) Cromer, D. T.; Waber, J. T. "International Tables for X-ray Crystallography"; Kynoch Press: Birmingham, England, 1974; Vol. IV, Table 2.2A.
(19) Stewart, R. F.; Davidson, E. R.; Simpson, W. T. *J. Chem. Phys.* **1965**, *42*, 3175.
(20) Cromer, D. T.; Liberman, D. *J. Chem. Phys.* **1970**, *53*, 1891.
(21) $R = \sum||F_o| - |F_c||/\sum|F_o|$; $R_w = [\sum w(|F_o| - |F_c|)^2/\sum wF_o^2]^{1/2}$.

Table III. Positional and Thermal Parameters for the Nongroup Atoms of *trans*-$[Rh_2Cl_2(CO)_2(DPM)_2]$

atom	x^a	y	z	$U_{11}{}^b$	U_{22}	U_{33}	U_{12}	U_{13}	U_{23}
Rh	−0.02710 (2)	0.04223 (2)	−0.15345 (2)	2.36 (2)	2.13 (2)	2.83 (2)	−0.67 (1)	1.26 (1)	0.08 (1)
Cl	−0.18334 (9)	−0.06132 (8)	−0.2207 (1)	3.63 (5)	3.77 (5)	4.22 (5)	−1.76 (4)	1.70 (4)	−0.16 (4)
P(1)	−0.22241 (9)	0.20635 (7)	−0.13917 (9)	2.63 (5)	2.20 (4)	3.00 (5)	−0.64 (3)	1.32 (4)	0.24 (3)
P(2)	−0.17744 (9)	0.12221 (7)	0.15280 (9)	2.48 (4)	2.34 (4)	2.90 (5)	−0.69 (3)	1.32 (4)	−0.01 (3)
O	0.1297 (4)	0.1852 (3)	−0.1355 (4)	7.1 (2)	4.4 (2)	10.3 (3)	−2.9 (2)	5.8 (2)	−0.9 (2)
C(1)	0.0725 (4)	0.1309 (3)	−0.1376 (5)	3.4 (2)	5.6 (3)	5.6 (3)	−1.0 (2)	2.4 (2)	−1.2 (2)
C(2)	−0.3019 (3)	0.1785 (3)	−0.0309 (4)	2.6 (2)	2.7 (2)	2.9 (2)	−0.7 (1)	1.5 (1)	−0.2 (1)

[a] Estimated standard deviations in the least significant figure are given in parentheses in this and all subsequent tables. [b] The form of the anisotropic thermal ellipsoid is $\exp[-2\pi^2(a^{*2}U_{11}h^2 + b^{*2}U_{22}k^2 + c^{*2}U_{33}l^2 + 2a^*b^*U_{12}hk + 2a^*c^*U_{13}hl + 2b^*c^*U_{23}kl)]$. The quantities given in the table are the thermal coefficients × 10^2.

Table IV

Derived Parameters for Rigid-Group Atoms of *trans*-$[Rh_2Cl_2(CO)_2(DPM)_2]$

atom	x	y	z	B, Å^2	atom	x	y	z	B, Å^2
C(11)	−0.2018 (3)	0.3442 (2)	−0.0656 (3)	2.48 (6)	C(31)	−0.1562 (3)	0.2475 (2)	0.2675 (3)	2.43 (6)
C(12)	−0.3189 (2)	0.4518 (2)	−0.1109 (2)	3.66 (8)	C(32)	−0.0330 (3)	0.2239 (2)	0.3966 (2)	3.61 (7)
C(13)	−0.3039 (2)	0.5548 (2)	−0.0460 (2)	4.71 (9)	C(33)	−0.0182 (4)	0.3131 (3)	0.4952 (2)	4.94 (9)
C(14)	−0.1719 (3)	0.5503 (2)	0.0641 (3)	4.86 (9)	C(34)	−0.1265 (3)	0.4259 (2)	0.4648 (3)	4.64 (9)
C(15)	−0.0549 (2)	0.4428 (2)	0.1094 (2)	4.34 (8)	C(35)	−0.2496 (3)	0.4495 (2)	0.3357 (2)	4.57 (9)
C(16)	−0.0698 (2)	0.3397 (2)	0.0445 (2)	3.09 (7)	C(36)	−0.2645 (4)	0.3603 (3)	0.2371 (2)	3.33 (7)
C(21)	−0.3759 (6)	0.2513 (2)	−0.3145 (2)	2.51 (6)	C(41)	−0.2962 (4)	0.0928 (3)	0.2113 (6)	2.25 (6)
C(22)	−0.5019 (5)	0.2311 (3)	−0.3546 (4)	3.10 (7)	C(42)	−0.4395 (5)	0.1074 (2)	0.1225 (4)	2.86 (6)
C(23)	−0.6134 (4)	0.2652 (3)	−0.4909 (3)	3.92 (8)	C(43)	−0.5214 (2)	0.0819 (2)	0.1747 (2)	3.29 (7)
C(24)	−0.5989 (6)	0.3194 (2)	−0.5870 (2)	4.30 (8)	C(44)	−0.4600 (4)	0.0420 (3)	0.3157 (6)	3.29 (7)
C(25)	−0.4728 (5)	0.3396 (3)	−0.5469 (4)	4.54 (9)	C(45)	−0.3166 (5)	0.0274 (2)	0.4045 (4)	3.83 (8)
C(26)	−0.3614 (4)	0.3055 (3)	−0.4107 (3)	3.67 (8)	C(46)	−0.2347 (2)	0.0529 (2)	0.3524 (2)	3.40 (7)

Rigid-Group Parameters

group	$X_c{}^a$	Y_c	Z_c	δ^b	ϵ	η
ring 1	−0.1868 (2)	0.4473 (2)	−0.0007 (2)	−0.231 (2)	2.822 (2)	4.892 (1)
ring 2	−0.4874 (2)	0.2854 (2)	−0.4508 (2)	0.916 (2)	2.384 (3)	3.127 (3)
ring 3	−0.1413 (2)	0.3367 (2)	0.3662 (2)	2.683 (2)	2.597 (2)	1.198 (2)
ring 4	−0.3781 (2)	0.0674 (1)	0.2635 (2)	4.237 (2)	2.366 (3)	4.823 (3)

[a] X_c, Y_c, and Z_c are the fractional coordinates of the centroid of the rigid group. [b] The rigid-group angles δ, ϵ, and η (rad) are the angles by which the rigid body is rotated with respect to a set of axes X, Y, and Z. The origin is the center of the ring; X is parallel to a^*, Z is parallel to c, and Y is parallel to the line defined by the intersection of the plane containing a^* and b^* with the plane containing b and c.

Table V. Selected Distances (Å) in *trans*-$[Rh_2Cl_2(CO)_2(DPM)_2]$

Bonded			
Rh-Cl	2.3875 (9)	P(1)-C(11)	1.833 (2)
Rh-P(1)	2.3141 (9)	P(1)-C(21)	1.831 (2)
Rh-P(2)'[a]	2.3315 (9)	P(2)-C(31)	1.834 (2)
Rh-C(1)	1.814 (4)	P(2)-C(41)	1.842 (2)
P(1)-C(2)	1.840 (3)	C(1)-O	1.102 (5)
P(2)-C(2)	1.835 (3)		
Nonbonded			
Rh-Rh'	3.2386 (5)	O-H(14)[c]	2.56
Rh-Cl'	3.569 (1)	C(1)-H(16)'	2.69
P(1)-P(2)	3.130 (1)	C(2)-H(42)	2.57
Cl-H(16)	2.69	C(2)-H(22)	2.64
Cl-H(45)[b]	2.73		

[a] Primed atoms related to unprimed atoms by a center of inversion in this and all subsequent tables. [b] Atom located at $\bar{x}$, $\bar{y}$, $1-z$. [c] Atom located at x, $y-1$, z.

Discussion

(a) Description of Structure. The structure of *trans*-$[Rh_2Cl_2(CO)_2(DPM)_2]$, shown in Figure 1, consists of one discrete dimeric unit located on the inversion center at the origin. The molecule therefore has crystallographically imposed $\bar{1}$ symmetry. There are no unusually short intermolecular contacts (Table V). Figure 2 presents a perspective view of the molecule including the numbering scheme (phenyl hydrogen atoms have the same number as their attached carbon atoms). The inner coordination sphere is shown in Figure 3 along with the relevant bond lengths.

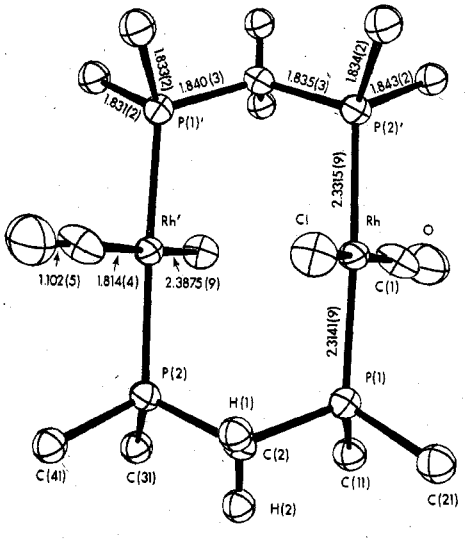

Figure 3. The inner coordination sphere of *trans*-$[Rh_2Cl_2(CO)_2(DPM)_2]$ showing some relevant bond lengths. Only the first carbon atom of each phenyl ring is shown. 50% thermal ellipsoids are drawn.

The coordination about each Rh atom is effectively square planar with trans geometry about each metal, much like Vallarino's compound and its analogues.[23,24] Slight tetrahedral distortions of the square plane are evident as was observed in

(22) Supplementary material.

(23) DeBoer, J. L.; Rogers, D.; Skapski, A. C.; Troughton, P. G. H. *Chem. Commun.* **1966**, 756.
(24) Vallarino, L. *J. Chem. Soc.* **1957**, 2287.

Table VI. Selected Angles (Deg) in *trans*-$[Rh_2Cl_2(CO)_2(DPM)_2]$

Bond Angles			
Cl-Rh-P(1)	86.20 (3)	C(2)-P(1)-C(11)	102.7 (1)
Cl-Rh-P(2)′	95.33 (3)	C(2)-P(1)-C(21)	103.2 (1)
Cl-Rh-C(1)	169.1 (1)	C(2)-P(2)-C(31)	107.8 (1)
C(1)-Rh-P(1)	91.6 (1)	C(2)-P(2)-C(41)	101.8 (1)
C(1)-Rh-P(2)′	87.5 (1)	C(11)-P(1)-C(21)	103.1 (1)
P(1)-Rh-P(2)′	176.50 (2)	C(31)-P(2)-C(41)	99.5 (1)
Rh-C(1)-O	176.3 (4)	P(1)-C(11)-C(12)	121.0 (1)
P(1)-C(2)-P(2)	116.8 (2)	P(1)-C(11)-C(16)	118.9 (1)
Rh-P(1)-C(2)	112.2 (1)	P(1)-C(21)-C(22)	122.8 (1)
Rh-P(2)′-C(2)′	110.9 (1)	P(1)-C(21)-C(26)	117.1 (1)
Rh-P(1)-C(11)	121.22 (8)	P(2)-C(31)-C(32)	117.3 (1)
Rh-P(1)-C(21)	112.39 (9)	P(2)-C(31)-C(36)	122.4 (1)
Rh-P(2)′-C(31)′	120.35 (8)	P(2)-C(41)-C(42)	123.6 (1)
Rh-P(2)′-C(41)′	114.53 (9)	P(2)-C(41)-C(46)	116.4 (1)
Torsion Angles			
P(1)-Rh-Rh′-P(2)	2.19 (3)	C(1)-Rh-P(1)-C(2)	140.6 (2)
Cl-Rh-P(1)-C(2)	−50.1 (1)	C(1)-Rh-P(1)-C(11)	18.9 (2)
Cl-Rh-P(1)-C(11)	−171.7 (1)	C(1)-Rh-P(1)-C(21)	−103.5 (2)
Cl-Rh-P(1)-C(21)	65.74 (9)	C(1)-Rh-P(2)′-C(2)′	−90.8 (2)
Cl-Rh-P(2)′-C(2)′	99.7 (1)	C(1)-Rh-P(2)′-C(31)	142.2 (2)
Cl-Rh-P(2)′-C(31)′	−27.2 (1)	C(1)-Rh-P(2)′-C(41)′	23.7 (2)
Cl-Rh-P(2)′-C(41)′	−145.73 (9)		
Vector-Plane Normal Angles			
Rh-Rh′,Rh-Cl-P(1)	12.98 (2)	Rh-Rh′,Rh-C(1)-P(2)′	23.6 (1)

the red and orange forms of Wilkinson's compound.[25] Therefore the two phosphorus atoms are folded toward each other in the direction of the Rh–Rh vector whereas the Cl and CO ligands are folded in the opposite direction (Table VI). The dimeric unit is composed of two of these parallel square planes in an eclipsed conformation and bridged by the diphosphine ligands. These planes are arranged such that the chloro ligands on adjacent rhodium atoms are mutually trans, as are the carbonyl ligands. Significantly, the square planes are not perpendicular to the Rh–Rh vector but are inclined to it by ca. 75.9° (Table VII) with the chloro ligands folded in toward the bridging sites between the metal centers. This same twist of the Rh square planes is also observed in *trans*-$[Rh_2Cl_2(CO)_2(DAM)_2]$, although it was not noted in the original report on this compound.[13] The skewing of these planes seems to result from an attempt to minimize the nonbonded contacts between the equatorial chloro and carbonyl ligands and the phenyl rings. So in the observed conformation the Rh–Cl and Rh–CO vectors are staggered with respect to the P–C vectors (Table VI).

Within the Rh–DPM framework the parameters are essentially as observed in other similar DPM-bridged complexes.[1,3,5,6,13,26] The two independent Rh–P distances (2.3141 (9) and 2.3315 (9) Å) are significantly different; however, no chemical significance is attached to this difference. More likely the difference is a consequence of packing considerations (vide infra). Unlike most other DPM-bridged species which have a cis methylene arrangement, the methylene groups in the present compound are folded in a trans configuration with the methylene carbon atoms displaced by 0.720 (4) Å from the best intraligand Rh–P–P–Rh planes. The folding of the methylene carbon atoms out of these planes occurs such that the phenyl groups avoid the equatorial ligands.

The parameters involving the chloro and carbonyl ligands are not unusual, being typical for Rh(I) phosphino complexes.[2,5,13,23,25,26]

The relatively long Rh···Rh separation of 3.2386 (5) Å is consistent with no formal metal–metal bond and is in fact significantly longer than the nonbonded Rh–Rh separations of 3.1520 (8) and 3.155 (4) Å observed in $[Rh_2(CO)_2(\mu\text{-}Cl)(DPM)_2][BF_4]$[5] and $[Rh_2(CO)_2(\mu\text{-}S)(DPM)_2]$,[26] respectively. In these two "A-frame" species the metal centers are held closer than in the present structure owing to the constraints of the bridging chloro and sulfido ligands, respectively, in the former two species. As in previous determinations in which no metal–metal bond was present the intraligand P···P separation (3.130 (1) Å) is significantly less than the Rh–Rh separation. However the Rh–Rh separation is still considerably less than that observed in the DAM analogue (3.396 (1) Å),[13] reflecting the differences in bite size of the two ligands. A further indication that the Rh–Rh interaction, in the present compound, is repulsive is seen in a comparison of the P–C–P (116.8 (2)°) and As–C–As (113.5 (4)°) angles in the DPM and DAM[13] complexes, respectively. The larger P–C–P angle reflects the strain on the DPM ligand as the metal centers are tending apart.

A comparison of the metrical parameters of the DPM and DAM ligands in the present complex and in *trans*-$[Rh_2Cl_2(CO)_2(DAM)_2]$,[13] respectively, shows the expected trend, resulting from the larger covalent radius of As compared to P. Therefore the average $P\text{–}C_{methylene}$ (1.838 (4) Å),[27] $P\text{–}C_{phenyl}$ (1.835 (5) Å), and Rh–P (2.32 (1) Å) distances are all significantly less than the corresponding $As\text{–}C_{methylene}$ (1.97 (2) Å), $As\text{–}C_{phenyl}$ (1.936 (9) Å), and Rh–As (2.407 (4) Å) distances.

The primary reason for undertaking the structural determination of *trans*-$[Rh_2Cl_2(CO)_2(DPM)_2]$ was to permit comparisons between it and the analogous DAM complex in order to gain an understanding of the differences in their solubilities and chemistries. Based on the packing of the complex, shown in Figure 1, it is not difficult to understand the insolubility of the DPM complex. All the phenyl rings in the lattice have one of essentially two orientations, allowing extremely efficient packing of the molecules and efficient stacking of the parallel phenyl rings. Since the DPM complex turns out to be essentially isostructural with the DAM analogue,[13] we find the solubility differences somewhat surprising. We assume therefore that the subtle differences resulting from the larger Rh(DAM) framework (vide supra) results in less efficient packing than in the DPM complex. The effect of the larger molecular framework is obvious in the cell parameters which result in the unit cell volume of the DAM complex being ca. 4% larger than that of the DPM complex. Studies are now under way to unambiguously establish the nature of the species which we proposed[3,6] is the cis isomer of complex **1**, *cis*-$[Rh_2Cl_2(CO)_2(DPM)_2]$, in order to determine the reasons for the chemical differences between it and the trans analogue.

As we had expected, the Rh–Rh separation in the DPM complex is significantly shorter than that in the DAM complex. It is anticipated that the different ligand bites will have significant effects on the stabilities of ketonic carbonyl species, which contain bridging carbonyl ligands but no metal–metal bond. Certainly studies to date do indicate a difference in stability between DPM and DAM ketonic carbonyl species, although these effects are opposite with Rh[8] compared to Pd[10] and Pt.[11] The present structure and that of complex **2**[13] conclusively establish the significantly different effects that the DPM and DAM ligands have in establishing metal–metal separations, and we anticipate that the structural comparisons of these two complexes will prove useful in explaining the stabilities of ketonic carbonyl species when more such information is available.

(b) Halide-Exchange Reactions. The very close similarity in the structures of the DPM- and DAM-*trans*-dichlorodi-

(25) Bennett, M. J.; Donaldson, P. B.; Hitchcock, P. B.; Mason, R. *Inorg. Chim. Acta* **1975**, *12*, L9; Bennett, M. J.; Donaldson, P. B. *Inorg. Chem.* **1977**, *16*, 655.

(26) Kubiak, C. P.; Eisenberg, R. *J. Am. Chem. Soc.* **1977**, *99*, 6129.

(27) For averaged quantities the estimated standard deviation shown is the larger of an individual standard deviation or the standard deviation of a single observation as calculated from the mean.

Table VII

Least-Squares Plane Calculations

plane	equation	plane	equation
1	$-0.7174X - 0.5092Y - 0.4755Z + 0.0 = 0.0$[a]	2	$0.1832X + 0.1661Y - 0.9689Z + 1.5689 = 0.0$

Deviations from the Planes (Å)

	atom							
plane	Rh	P(1)	P(2)	P(2)'	Cl	C(1)	O	C(2)
1	−0.0047 (2)	−0.040 (1)	0.040 (1)					0.720 (4)[b]
2	−0.0021 (2)	0.0637 (9)		0.0608 (9)	−0.0492 (9)	−0.302 (4)	−0.553 (4)	

Dihedral Angle between Planes 1 and 2 = 75.9°

[a] *X*, *Y*, and *Z* are orthogonal coordinates (Å) with *X* along the *a* axis, *Y* in the *a*–*b* plane, and *Z* along the *C** axis. [b] Not included in least-squares plane calculation.

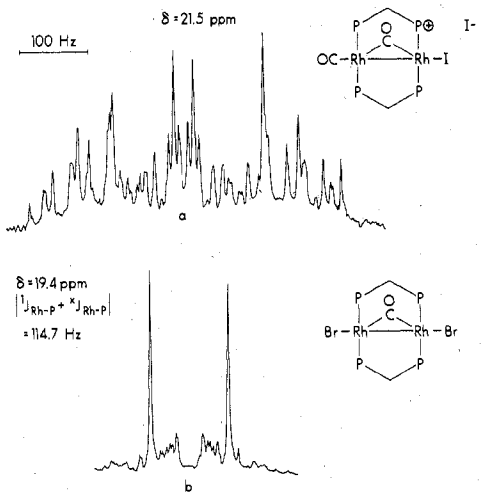

Figure 4. The $^{31}P\{^1H\}$ NMR spectra at −50 °C of (a) $[Rh_2I(\mu\text{-}CO)(CO)(DPM)_2][I]$ and (b) $[Rh_2Br_2(\mu\text{-}CO)(DPM)_2]$.

carbonyl species (**1** and **2**, respectively) was somewhat surprising; we had expected differences in the chloro and carbonyl ligand orientations. The products of the halide-exchange reactions however *do* show interesting structural and chemical trends which seem to depend on the steric bulk of the halide ligands and also on the crowding at the two metal centers as governed by the bridging DPM and DAM groups.

The reaction of complex **1** with NaBr yields initially $[Rh_2Br(\mu\text{-}CO)(CO)(DPM)_2][Br]$ (**3**), a species with bands in the infrared spectrum at 1958 and 1800 cm^{-1}, consistent with terminal and bridging carbonyl ligands. This species is a 1:1 electrolyte in acetone,[28] and its $^{31}P\{^1H\}$ NMR spectrum, which is similar to that of the iodo species, **5** shown in Figure 4 (vide infra), indicates an asymmetric species. This evidence coupled with the elemental analysis leads to the formulation of **3** as shown. In solution complex **3** recoordinates Br^- and

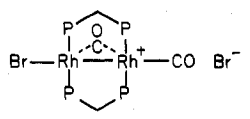

3

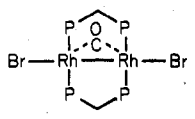

4b

undergoes CO loss, over a period of several hours, to yield $[Rh_2Br_2(\mu\text{-}CO)(DPM)_2]$ (**4b**), which has been characterized by an X-ray structure determination.[29] The $^{31}P\{^1H\}$ NMR spectrum of this species is shown in Figure 4 and is consistent with the symmetric structure observed in the solid state. All $^{31}P\{^1H\}$ NMR parameters (Table I) are in excellent agreement with those of the analogous species $[Rh_2X_2(\mu\text{-}L)(DPM)_2]$ (X = Cl, Br; L = SO_2, CS_2).[6,8] A solution of **4b** is nonconducting. The analogous chloro complex, $[Rh_2Cl_2(\mu\text{-}CO)(DPM)_2]$ (**4a**) is obtained on refluxing a suspension of the *trans*-dichlorodicarbonyl species **1**. This reaction has also been observed by Balch and co-workers,[30] although it is not clear whether the species isolated by these workers is identical with the one which we observe.

The reaction of **1** with KI yields $[Rh_2I(\mu\text{-}CO)(CO)(DPM)_2][I]$ (**5**), analogous to complex **3**. The carbonyl bands in the infrared spectrum are observed at 1955 and 1810 cm^{-1} and the $^{31}P\{^1H\}$ NMR spectrum (Figure 4) is consistent with the asymmetric structure proposed. Complex **5** is a 1:1 electrolyte in solution. Unlike complex **3** however, complex **5** is stable under N_2 in solution and does not undergo CO loss.

The bromo–DAM species, $[Rh_2Br_2(CO)_2(DAM)_2]$, is known and is probably structurally similar to the *trans*-dichlorodicarbonyl–DAM species (**2**).[12] Iodide exchange on complex **2** yields a species which infrared studies and elemental analysis indicate is probably a mixture of the *trans*-diiododicarbonyl complex *trans*-$[Rh_2I_2(CO)_2(DAM)_2]$ (**6**) and an asymmetric species $[Rh_2I(\mu\text{-}CO)(CO)(DAM)_2][I]$ (**7**), which is probably similar to the DPM species **5**. The asymmetric species in this mixture is more dominant.

The structural trend observed in the above series of DPM and DAM halides is therefore consistent with steric bulk arguments indicating that the trans configuration of equatorial ligands, as observed in the dichloro species **1** and **2**, and probably in $[Rh_2Br_2(CO)_2(DAM)_2]$, is destabilized with bulkier halide ligands. The larger steric bulk of the bromo ligand, compared to chloro, does not favor the simultaneous coordination of both bromo and both carbonyl ligands in the DPM complex, so the asymmetric, ionic species is initially formed. When bromide recoordination does occur, it is accompanied by CO loss to give the monocarbonyl species **4b**. With the DPM ligand, the stable iodo species is the asymmetric complex **5**, again because simultaneous coordination of all iodo and carbonyl ligands is not favored owing to steric crowding. Furthermore, the large size of I^- does not permit its recoordination so CO loss is not observed in this species. The effect of the larger DAM ligand is seen in the bromo DAM species which still exists as the *trans*-dibromodicarbonyl complex, unlike the DPM analogue. The DAM ligand presumably allows more room to accommodate the larger bromo ligands. Even with the bulkier iodo ligand some *trans*-diiododicarbonyl complex **6** is observed together with the asymmetric species **7**.

(c) Reactions with CO. (i) Dicarbonyl Species. It is interesting that no evidence is seen for the symmetric "A-frame" species **8** (X = Br, I), even though reactions of **3** and **5** with

(28) The maximum conductivity obtained was $\Lambda = 50\ \Omega^{-1}\cdot cm^2\cdot mol^{-1}$. However this compound can not be isolated pure being always contaminated by the neutral species $[Rh_2Br_2(\mu\text{-}CO)(DPM)_2]$.

(29) Cowie, M. C.; Dwight, S. K. *Inorg. Chem.*, in press.

(30) Balch, A. L., personal communication.

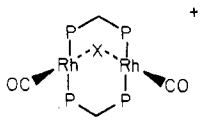

8

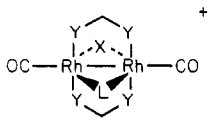

9, L = CO, Y = P
10, L = SO_2, Y = P
11, L = CO, Y = As, X = I
12, L = SO_2, Y = As, X = I

CO and SO_2 yield species **9** and **10**, respectively, which are analogous to the products obtained (**9a** and **10a**) by the reaction of **8a** (X = Cl) with these small molecules.[1-3,6,31] The $^{31}P\{^1H\}$ NMR spectra of the tricarbonyl species **9b** and **9c** (X = Br and I, respectively; L = CO) show one phosphine environment and are extremely similar to that of the chloro analogue, $[Rh_2(CO)_2(\mu\text{-}CO)(\mu\text{-}Cl)(DPM)_2]^+$ (**9a**) whose structure has been determined.[1,2] These DPM tricarbonyl complexes show an interesting trend in ^{31}P shifts and coupling constants (for Cl, Br, and I, δ 29.6, 28.7, and 26.6 ($|^1J_{Rh-P} + {}^xJ_{Rh-P}|$ = 94.2, 93.8, and 92.7 Hz), respectively). Furthermore, the infrared data for compounds **9a**, **9b**, and **9c** are all closely comparable. The complexes *trans*-$[Rh_2X_2(CO)_2(DAM)_2]$ (X = Cl, Br) like their DPM–chloro analogue (**1**), show no reaction with CO under our conditions. Reaction of a mixture of the iodo–DAM species **6** and **7** with CO, however, results in the isolation of a tricarbonyl species **11**, which appears from its infrared spectrum to be analogous to **9b** and **9c**.

An investigation of the ease of decarbonylation of complexes **9** shows a notable trend. The chloro complex **9a** readily loses CO in solution under an N_2 stream or in the solid state under vacuum;[1,31] the bromo species **9b** on the other hand does not lose CO in the solid state under vacuum even after 72 h but loses it slowly in solution to give complex **3** and subsequently complex **4b**. The iodo species **9c** does not lose CO either in the solid state or in solution. The DAM–iodo species **11** undergoes CO loss slowly in solution under an N_2 stream. On decarbonylation of the bromotricarbonyl species, **9b**, the complex initially produced is the asymmetric species **3**. This is consistent with the findings of Mague and co-workers[1,31] which indicate that in the chlorotricarbonyl complex, $[Rh_2(CO)_2(\mu\text{-}CO)(\mu\text{-}Cl)(DPM)_2]^+$, it is initially a terminal carbonyl ligand which is lost with the bridging carbonyl ligand then moving to the terminal site. With the assumption of the same mechanism for the bromo analogue, the intermediate species after CO loss would then be

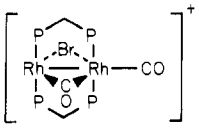

Owing to the large steric bulk of the bromo ligand it is this ligand which moves to the less sterically encumbered terminal site yielding species **3**, whereas with the chloro species migration of the carbonyl ligand is favored, presumably for electronic reasons.

(ii) Monocarbonyl Species. Reaction of $[Rh_2X_2(\mu\text{-}CO)(DPM)_2]$ (X = Cl (**4a**); X = Br (**4b**)) with excess CO results in the formation of the tricarbonyl species **9a** and **9b**. When the slow stepwise reaction of **4b** with CO is monitored by $^{31}P\{^1H\}$ NMR spectroscopy, resonances are observed which are assignable to the asymmetric dicarbonyl species **3** and to the tricarbonyl complex **9b**. Complex **3** is observed throughout the reaction but only in trace amounts. In contrast, the monocarbonyl species is found in significant quantities until completion of the reaction. It seems therefore that CO reacts preferentially with **3** compared to **4b**.

Scheme I. Reaction of $[Rh_2Cl_2(\mu\text{-}CO)(DPM)_2]$ with CO

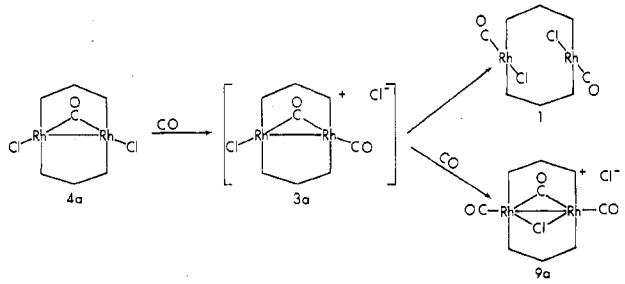

If instead of reacting **4a** with excess CO, the CO is added slowly, *trans*-$[Rh_2Cl_2(CO)_2(DPM)_2]$ (**1**) precipitates from solution (see Scheme I). This observation of two products (**1** and **9a**) from the slow and rapid addition of CO suggests the presence of an intermediate dicarbonyl species $[Rh_2Cl(\mu\text{-}CO)(CO)(DPM)_2][Cl]$ (**3a**), analogous to the bromo species **3**. We postulate that on slow CO addition attack of this intermediate by Cl^- occurs, giving complex **1**, whereas in the presence of excess CO (i.e., during rapid CO addition), attack by CO predominates, yielding instead the tricarbonyl species **9a**. On the basis of our other work with related "A-frame" species[6,29] and on a consideration of the electronic preference of each metal, we would predict that Cl^- attack on the intermediate species **3a** (Scheme I) occurs at the site between the bridging and terminal CO ligands, yielding a species

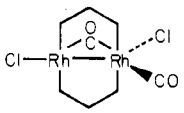

which could then readily rearrange to the *trans*-dichlorodicarbonyl species. Support of this postulated intermediate comes from the structural determination[32] of the analogous species which has $(MeO)_2PN(Et)P(OMe)_2$ instead of DPM ligands and which adopts this asymmetric geometry which we postulate for our dichlorodicarbonyl intermediate. Similarly if CO attacks species **3a** between the bridging CO and the chloro ligand, as we believe it does, complex **9a** is obtained by a facile shift of the chloro ligand into the bridging position.

(d) Reactions with SO_2. (i) Dicarbonyl Species. The ^{31}P NMR spectra of the SO_2 adducts **10b** and **10c** are consistent with one phosphine environment in each case and are similar to that obtained for $[Rh_2(CO)_2(\mu\text{-}SO_2)(\mu\text{-}Cl)(DPM)_2]^+$ (**10a**)[6] (for Cl, Br, and I, δ 24.6, 27.0, and 26.0 ($|^1J_{Rh-P} + {}^xJ_{Rh-P}|$ = 91.6, 90.6, and 90.3 Hz), respectively). In addition the infrared spectra of **10b** and **10c** are comparable to that of **10a**, leading to the formulation of these species as shown previously. Preliminary studies with *trans*-$[Rh_2X_2(CO)_2(DAM)_2]$ (X = Cl, Br) indicate that these complexes react in a manner similar to that for *trans*-$[Rh_2Cl_2(CO)_2(DPM)_2]$ yielding initially $[Rh_2(CO)_2(\mu\text{-}SO_2)(\mu\text{-}X)(DAM)_2][X]$ and eventually undergoing CO loss yielding $[Rh_2X_2(\mu\text{-}SO_2)(DAM)_2]$. Similarly the iodo complexes **6** and **7** react with SO_2 to yield an SO_2 adduct, $[Rh_2(CO)_2(\mu\text{-}SO_2)(\mu\text{-}I)(DAM)_2][I]$ (**12**) analogous to the DPM complexes.

The bromo species, $[Rh_2(CO)_2(\mu\text{-}SO_2)(\mu\text{-}Br)(DPM)_2][Br]$ (**10b**), on prolonged SO_2 treatment, undergoes a decarbonylation reaction yielding $[Rh_2Br_2(\mu\text{-}SO_2)(DPM)_2]$ (**13b**), paralleling the chemistry previously reported for the chloro analogue.[6] In contrast, the iodo species **10c** does not undergo this reaction. Studies on the conversion of $[Rh_2(CO)_2(\mu\text{-}SO_2)(\mu\text{-}Cl)(DPM)_2][Cl]$ to $[Rh_2Cl_2(\mu\text{-}SO_2)(DPM)_2]$ indicated[6] that chloride ion coordination was required before CO

(31) Mague, J. T.; Sanger, A. R. *Inorg. Chem.* **1979**, *18*, 2060.

(32) Haines, R. J., personal communication.

Scheme II. A Possible Reaction Sequence for the Reaction of $[Rh_2Br_2(\mu\text{-}CO)(DPM)_2]$ with SO_2

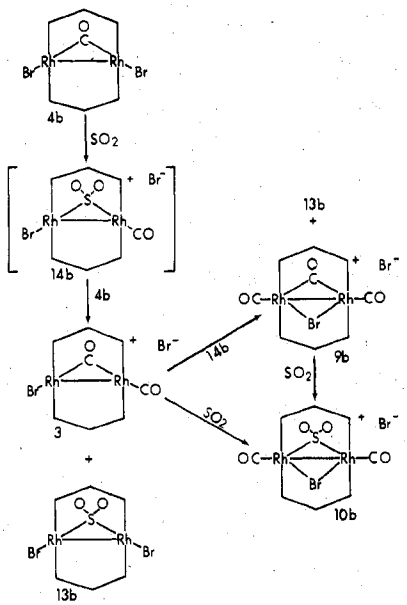

loss was observed so we assume that although Br^- coordination occurs in **10b**, the increased steric bulk of the iodo ligand prevents coordination of the second I^- ion in **10c** and therefore prevents subsequent CO loss.

Although SO_2 can be readily removed from species **10a**[3,6,29] this is not observed for complexes **10b** and **10c**. The bromo species **10b** instead undergoes CO loss in solution under N_2 flush to yield $[Rh_2Br_2(\mu\text{-}SO_2)(DPM)_2]$ (**13**), whereas **10c** loses neither CO nor SO_2.

(ii) Monocarbonyl Species. The reactions of $[Rh_2X_2(\mu\text{-}CO)(DPM)_2]$ (X = Cl (**4a**); X = Br (**4b**)) with SO_2 yield as the final products $[Rh_2X_2(\mu\text{-}SO_2)(DPM)_2]$ (**13a,b**) and $[Rh_2(CO)_2(\mu\text{-}SO_2)(\mu\text{-}X)(DPM)_2][X]$ (**10a,b**) for the chloro and bromo complexes. When these reactions are monitored, during the slow stepwise addition of SO_2, by utilizing $^{31}P\{^1H\}$ NMR spectroscopy, several unexpected products are obtained. The spectra of the reaction of **4b** with SO_2 show the presence of two asymmetric species (**3** and **14b**) and four symmetric species (**4b**, **9b**, **10b**, and **13b**) at different times during the experiment (see Scheme II). Of these species only **14b** has not been previously characterized by us. This species we tentatively assign as a monocarbonyl–mono(sulfur dioxide) species, possibly having the structure shown. This asymmetric structure is consistent with the $^{31}P\{^1H\}$ NMR pattern observed and the infrared data which show an SO_2 species with a terminal carbonyl ligand as one of the first products. Furthermore, it is not an unreasonable initial product in the reaction. All other species can be explained by CO transfer from this species to others present in solution. So although Scheme II is not meant to represent unambiguously the sequence of events, it does present some plausible steps in the production of the observed species and in particular offers explanations for the production of di- and tricarbonyl products from a monocarbonyl reactant. For example, CO transfer from **14b** to **4b** would yield **3** and one of the final products, **13b**. The other final product in the reaction, **10b**, can be obtained by the reaction of **3** with SO_2. Complex **3** can also react with **14b** yielding more **13b** and the tricarbonyl species **9b** which can subsequently react with SO_2 giving **10b**.

The analogous reaction of **4a** with SO_2 seems to proceed by a simpler route. Again an asymmetric species **14a** tentatively assigned as being analogous to the bromo species **14b** is observed in the NMR experiment. However, only two other species, **10a** and **13a**, are observed, resulting from CO transfer from one molecule of **14a** to another. There may be other intermediates in this reaction but none is observed.

Conclusions

We have seen in these halide complexes an interesting structural trend which is dependent on halide size and on the relative dimensions of the DPM and DAM ligands. The chemistries of these halide species with CO and SO_2 also show interesting trends which can again be attributed, at least, in part, to steric interactions between the ligands. Also notable in this chemistry is the strong tendency toward symmetric species. Only in the two iodo species **5** and **7**, where the steric bulk of the iodo ligand inhibits the chemistry favored by the other halide species, are the asymmetric species stable. Therefore the asymmetric complex $[Rh_2Br(\mu\text{-}CO)(CO)(DPM)_2][Br]$ either loses CO yielding the symmetric species $[Rh_2Br_2(\mu\text{-}CO)(DPM)_2]$ or gains CO to give another symmetric species $[Rh_2(CO)_2(\mu\text{-}CO)(\mu\text{-}Br)(DPM)_2][Br]$. This tendency toward symmetric species is commonly observed throughout our binuclear chemistry with the DPM and DAM ligands[6,33] but is in contrast to analogous complexes with the related methoxydiphosphazane ligand, $(MeO)_2PN(Et)P(OMe)_2$, which show a tendency toward asymmetric species.[32] Investigations are currently underway in attempts to establish the reasons for this observed trend toward symmetric species such that we can better understand differences in chemistries between these DPM and DAM species and the related methoxydiphosphazane complexes.

Acknowledgment. The authors thank the National Science and Engineering Research Council of Canada and the University of Alberta for financial support, the NSERC for a scholarship to S.K.D., Professors A. L. Balch and R. J. Haines for communicating their results prior to publication, and Dr. T. G. Southern for technical assistance in the reaction of compound **4a** with CO.

Registry No. **1**, 22427-58-3; **2**, 23299-75-4; **3**, 73680-36-1; **4a**, 73680-37-2; **4b**, 73687-53-3; **5**, 73680-38-3; **6**, 73680-39-4; **7**, 73680-40-7; **9a**, 71647-01-3; **9b**, 73687-54-4; **9c**, 73680-41-8; **10a**, 71646-99-6; **10b**, 73680-18-9; **10c**, 73680-19-0; **11**, 73680-42-9; **12**, 73680-20-3; **13a**, 69063-81-6; **13b**, 73680-21-4.

Supplementary Material Available: Tables VIII and IX, showing the idealized hydrogen parameters and the root-mean-square amplitudes of vibration of the individual atoms, respectively, and a listing of the observed and calculated structure amplitudes (17 pages). Ordering information is given on any current masthead page.

(33) Cowie, M. C.; Southern T. G. *J. Organomet. Chem.*, in press.